Investigations

Tomasz Pfeifer, Bogusław Czwórnóg

The Effect of Plasma Surfacing Parameters on the Geometry and Structure of Overlay Welds

Abstract: The article presents the course and results of tests concerning plasma-powder surfacing of steels used in the power sector. The tests, involving the use of Inconel 625 alloy-based powder, aimed to determine the effect of process variables on overlay weld geometry, penetration depth and overlay weld-parent metal stirring degree. The article presents the results of metallographic examinations obtained by light microscopy, including the structure of overlay welds and Heat Affected Zone as well as the hardness distribution in overlay welds and Heat Affected Zone.

Keywords: plasma-powder surfacing, overlay welds, Inconel 625 alloy-based powder,

DOI: *10.17729/ebis.2015.4/1*

Introduction

Since the early 1960s, welding technologies utilising a concentrated electric arc have established themselves in the manufacturing industry, with plasma cutting being one of the primary thermal cutting methods. Due to unquestionable advantages of a concentrated electric arc, both plasma welding and plasma–powder surfacing are increasingly commonly used when joining elements and applying surfaces of specific properties. Low-temperature plasma is formed as a result of forcedly increased density of ionised molecules in the electric arc column by contracting its diameter and, consequently, rising arc temperature. An increase in arc temperature and in electric field intensity is accompanied by an increase in the kinetic energy of molecules and by a higher arc ionisation degree (due to more frequent collisions of molecules being bombarded by electrons). Plasma arc advantages, increasing the popularity of plasma welding and surfacing in many industries, are the following:

- easy arc initiation due to the use of an auxiliary arc burning between the welding torch cathode and the plasma nozzle,
- high arc stability and low sensitivity to changes of the distance between the plasma welding torch and a material being processed, greatly facilitating manual and mechanised welding,
- high power density translating to deeper penetration, narrower weld and Heat Affected Zone, resulting in smaller thermal strains of elements being welded,

dr inż. Tomasz Pfeifer (PhD (DSc) Eng.) – Instytut Spawalnictwa, Welding Technologies Department;
dr inż. Bogusław Czwórnóg (PhD (DSc) Eng.) – Deputy Director of Instytut Spawalnictwa

– high flexibility in adjustment of parameters enabling significantly more efficient mechanised welding or surfacing,
– high quality, aesthetics and metallurgical purity of welds and overlay welds.

Plasma-powder surfacing consists in using a plasma arc to melt filler metal in the form of nickel, cobalt, iron or copper-based alloy metallic powder or ceramic powder of spherical grains (0.04-0.3 mm in size) and transferring molten filler metal onto a previously prepared element surface using a plasma arc. In plasma surfacing, the heat source is a concentrated electric arc burning between a non-consumable electrode placed in the plasma torch and the base material. The major advantages of plasma-powder surfacing are the following:

– high arc stability;
– high smoothness of a surfaced layer, thus small allowances for mechanical working;
– high metallurgical purity of overlay welds;
– wide range of thicknesses of layers made in one run.

Plasma-powder surfacing is used for repairing elements made of unalloyed, alloy and corrosion-resistant structural steels, cast steels and some grades of cast irons. The scope of applications includes surfacing of combustion engine valve faces with stellite powders, surfacing of elements exposed to intense abrasion (e.g. applied in mining and drilling) using Fe-Cr-based powders, preventive and repair surfacing of extrusion machine roll worms (plastic processing), and, recently, also surfacing of elements made of power engineering steel grades using nickel alloys. Due to the introduction of directives concerning the reduction of emissions from power plants and waste incineration plants, recent years have seen the increasingly common use of power units characterised by supercritical parameters. The combustion of waste and fossil fuels in industrial boilers produces flue gases containing highly aggressive chlorides and fluorides. Their destructive effect necessitates the use of appropriate protections against corrosion and erosion in exchanger pipes, radiant tubes and combustion chambers. Many publications state that this purpose is best served by nickel-based alloys such as Inconel 625, 686 and 825 [2-4]. This article presents technological tests and their results in relation to plasma–powder surfacing of 10CrMo9-10 steel using Inconel 625 alloy powder. The tests aimed to determine the effect of plasma arc current, powder feeding rate, surfacing rate, plasma gas flow rate and preheating temperature on the process of surfacing, geometry of overlay welds, penetration depth and content of the base material in the overlay weld as well as on the structure and hardness distribution in overlay welds and in HAZ.

Materials, Test Rig and Testing Methodology

The base material used in the process of plasma surfacing was a 12 mm thick sheet made of 10CrMo9-10 grade chromium–molybdenum, creep resistant, dual-phase (ferritic-pearlitic) steel intended for operation at higher temperatures in the power sector. Table 1 presents the chemical composition of the steel, whereas Figure 1 presents its microstructure.

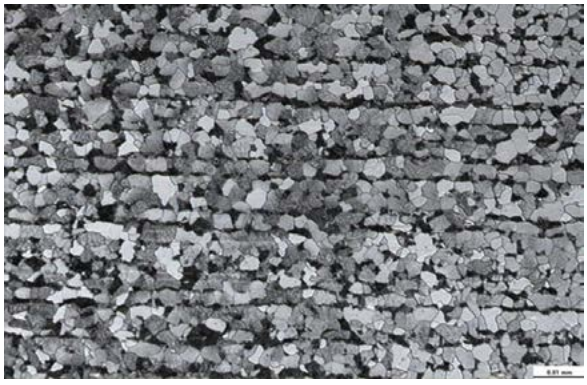

Fig. 1. Structure of the base material of 10CrMo9-10 steel, mag. 200 x., etchant: Nital

Table 1. Chemical composition of 10CrMo9-10 steel (% by weight) according to PN-EN 10216-2

C	Mn	Si	P	S	Cu	Cr	Ni	Mo	Al
0.08-0.14	0.3-0.7	max. 0.5	max. 0.025	max. 0.02	max. 0.3	2-2.5	max. 0.3	0.9-1.1	max. 0.04

The filler metal used in the tests was the Eu-Troloy 16625G-04 powder of Inconel 625 alloy composition manufactured by Messer Eutectic Castolin. The tests were performed on a test station equipped with a modern Castolin-made Eutronic Gap 3001 device. The welding torch along with the powder feeder were mounted on an automated MultiSurfacer D2 Weld station manufactured by Welding Alloys and provided with a microprocessor control system enabling the adjustment of a required direction and welding rate as well as ensuring the repeatable positioning of the torch (Fig. 2).

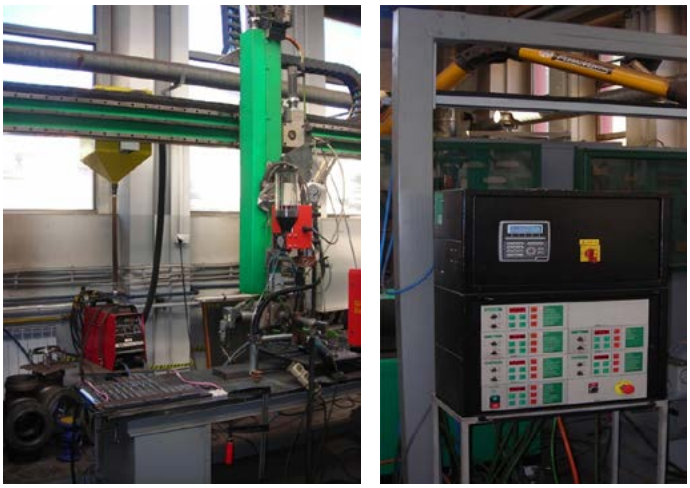

Fig. 2. Automated MultiSurfacer D2 Weld gantry for surfacing along with a control system, powder feeder and plasma torch

The testing methodology included surfacing technological tests performed using various process conditions and parameters. The technological tests were performed on specimens having the dimensions of 100×40×12 mm. On each specimen only one 80 mm long single-run overlay weld was made. Such an approach was adopted in order to ensure repeatable conditions and eliminate the heat effect of subsequent runs on the surfacing process and on the base material.

The first stage of the tests involved surfacing with low current values (100 A, 120 A and 150 A) and travel rate (20 cm/min), changing a powder mass feeding rate from 0.4 to 27 g/min. Next, current (100 A) and surfacing rates (20 cm/min) remained constant, a powder mass feeding rate changed within the range of 5.0-15.0 g/min and preheating to 200°C was used. At the subsequent stage, current (120 A) powder mass feeding rate (10.64 g/min) were constant and a travel rate changed from 10 to 105 cm/min. Afterwards, the same powder mass feeding rate and a constant travel rate of 30 cm/min were sued whereas current varied between 80 and 150 A.

Afterwards, each specimen was cut in half, transversely to the direction of surfacing (perpendicularly to the overlay weld axis) and macroscopic metallographic tests were performed. The etchant used in the tests was the Adler's reagent. Each overlay weld was digitally photographed. Afterwards, AutoCad 2013 graphic software was used to measure the geometry of overlay welds (width, height and penetration depth) and to determine the content of the base material in the overly weld (proportion between the area of penetration into the material and the whole overlay weld area). Figure 3 presents the manner used for the determination of the overlay weld geometry and the content of the base material in the overlay weld.

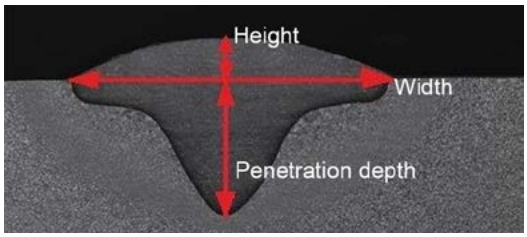

Fig. 3. Manner of determining the overlay weld geometry and penetration depth

The subsequent stage involved microscopic metallographic tests using a NiconEclipse Ma200 light microscope. Hardness measurements in the overlay weld and in the HAZ were performed under a nominal load of 98.1N (HV10) using a – KB50BYZ-FA hardness tester manufactured by KB Prüftechnik. The test results are presented below.

Test Results

Macroscopic metallographic images of selected overlay welds, obtained during the technological tests, are presented in Figures 4-6. The

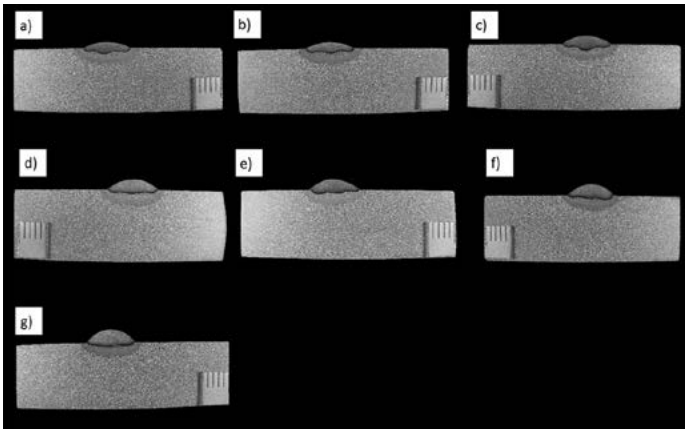

Fig. 4. Macrostructure of the overlay welds made using the constant value of current (120 A) and constant surfacing rate (20 cm/min) and various value of powder mass feeding rate, in g/min: 10.64(a); 12.64 (b); 14.60 (c); 16.44 (d); 18.55 (e); 20.8 (f); 22.82 (g) respectively

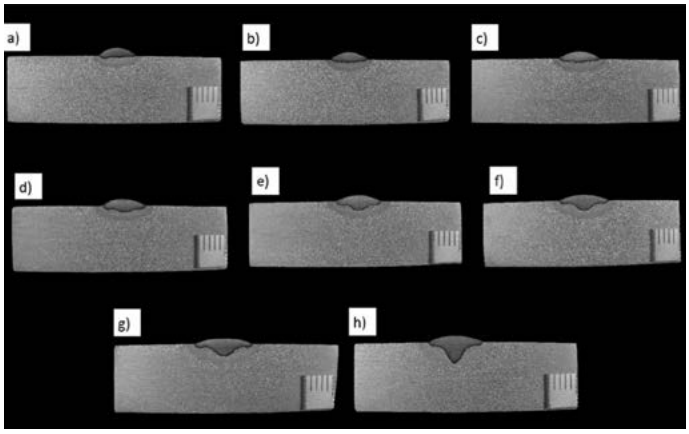

Fig. 5. Macrostructure of the overlay welds made using the constant value of powder mass feeding rate (10.64 g/min), constant surfacing rate (30 cm/min) and various value of current, in A: 80 (a), 90 (b), 100 (c), 110 (d), 120 (e), 130 (f), 140 (g), 150 (h) respectively

photographs were grouped in a manner enabling the presentation of overlay welds made with only one parameter changed (powder mass feeding rate, welding rate, plasma arc current). Figure 4 presents the macrostructures of overlay welds made with various powder mass feeding rates; Figure 5 presents the macrostructures of overlay welds made with various current values, and Figure 6 presents the macrostructures of overlay welds made with various surfacing rates.

The microscopic metallographic tests (light microscopy) were performed on the specimens surfaced using current of 100 A, welding rate of 20 cm/min and powder mass feeding rate of 5 g/min as well as the specimens made using the same parameters but previously preheated to 200°C. The tests were also performed on the specimens made using a) constant powder mass feeding rate and constant surfacing rate but various current and b) constant welding rate, constant current and various powder mass feeding rate. The tests aimed to determine the structure of the HAZ and of overlay welds as well as to determine the effect of preheating, powder mass feeding rate and current on the structure of the material in the Heat Affected Zone and on the

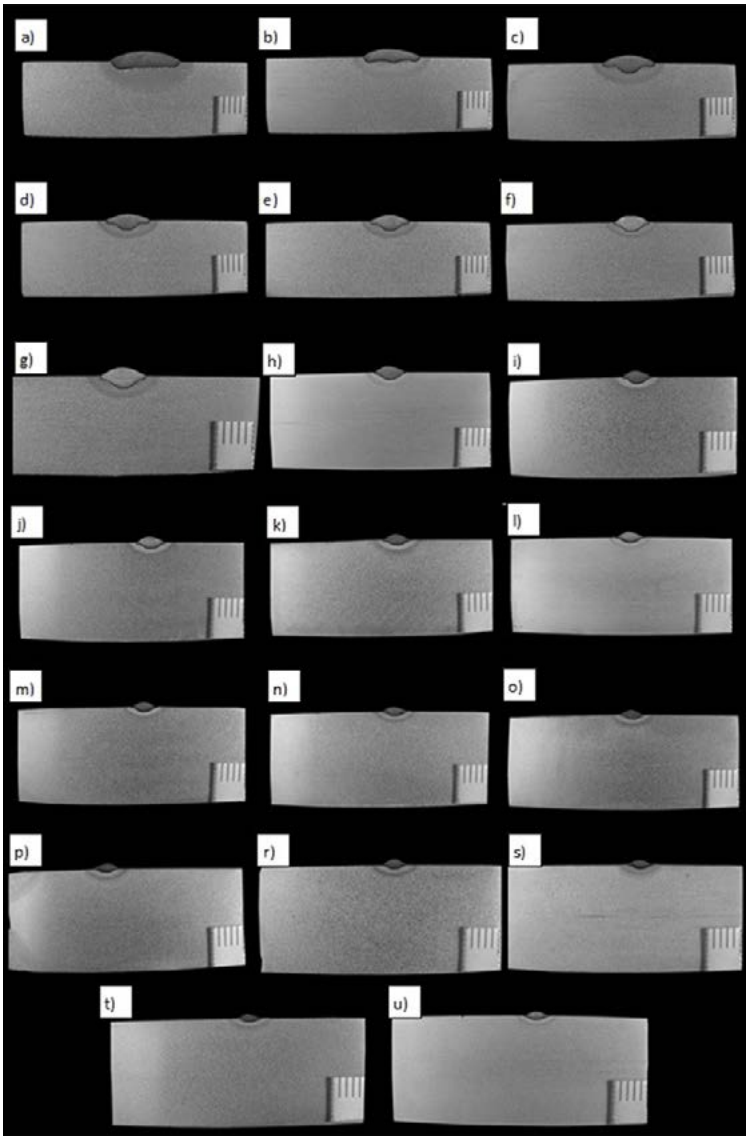

Fig. 6. Macrostructure of the overlay welds made using the constant value of powder mass feeding rate (10.64 g/min), constant value of current (120 A) and various value of surfacing rate, in cm/min: 10 (a), 15 (b); 20 (c); 25 (d); 30 (e); 35 (f), 40 (g), 45 (h), 50 (i), 55 (j), 60 (k), 65 (l), 70 (m), 75 (n), 80 (o), 85 (p), 90 (r), 95 (s), 100 (t), and 105 (u) respectively

Fig. 7. Microstructure of the Heat Affected Zone of 10CrMo9-10 steel subjected to plasma surfacing using Inconel 625 alloy and the following process parameters: current of 100 A, surfacing rate of 20 cm/min and powder mass feeding rate 5 g/min, etchant: Nital, mag. 500 x

structure of overlay welds. Metallographic tests performed at a magnification between 100 and 1000x were focused on observing the Heat Affected Zone at the overlay toe angle and at the greatest depth of penetration into the base material. Figures 7-13 present selected microscopic metallographic images.

Afterwards, selected plasma-surfaced overlay welds were subjected to the Vickers hardness test. The specimens selected for the test were made using technological parameters varying in powder mass feeding rates, surfacing rates and current, and in the use of preheating.

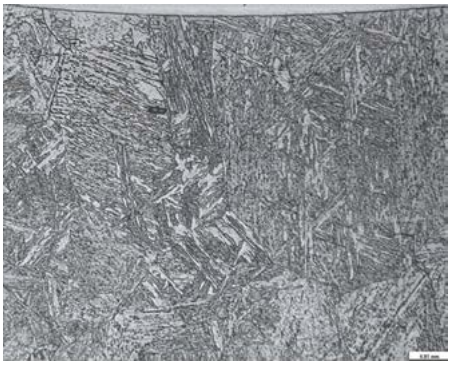

Fig. 8. Microstructure of the Heat Affected Zone of 10CrMo9-10 steel subjected to plasma surfacing using Inconel 625 alloy and the following process parameters: current of 100 A, surfacing rate of 20 cm/min and powder mass feeding rate 5 g/min, preheating to 200° etchant: Nital, mag. 500 x

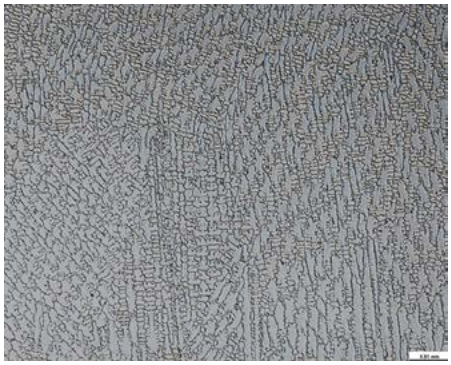

Fig. 9. Microstructure of the overlay weld made on 10CrMo9-10 steel using plasma surfacing and Inconel 625 alloy as well as the following process parameters: current of 100 A, surfacing rate of 20 cm/min and powder mass feeding rate 5 g/min, electrolytic etching, mag. 200 x

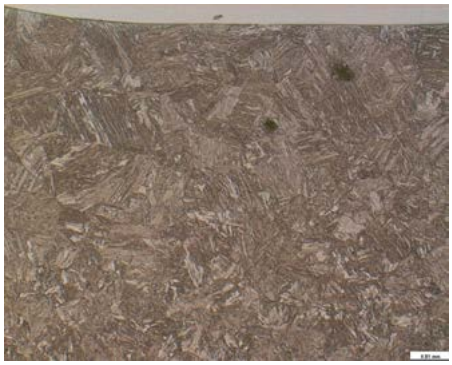

Fig. 10. Microstructure of the Heat Affected Zone of 10CrMo9-10 steel subjected to plasma surfacing using Inconel 625 alloy and the following process parameters: current of 90 A, surfacing rate of 30 cm/min and powder mass feeding rate 10.64 g/min, etchant: Nital, mag. 200 x

Fig. 11. Microstructure of the Heat Affected Zone of 10CrMo9-10 steel subjected to plasma surfacing using Inconel 625 alloy and the following process parameters: current of 150 A, surfacing rate of 30 cm/min and powder mass feeding rate 10.64 g/min, etchant: Nital, mag. 200 x

Fig. 12. Microstructure of the overlay weld made on 10CrMo9-10 steel using plasma surfacing and Inconel 625 alloy as well as the following process parameters: current of 90 A, surfacing rate of 30 cm/min and powder mass feeding rate 10.64 g/min, electrolytic etching, mag. 200 x

Fig. 13. Microstructure of the overlay weld made on 10CrMo9-10 steel using plasma surfacing and Inconel 625 alloy as well as the following process parameters: current of 150 A, surfacing rate of 30 cm/min and powder mass feeding rate 10.64 g/min, electrolytic etching, mag. 200 x

The diagram presenting the arrangement of measurement points is presented in Figure 14, whereas hardness test results are presented in Table 2.

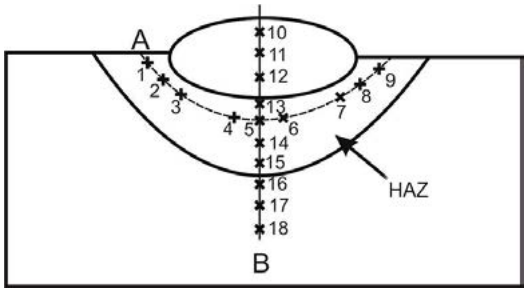

Fig. 14. Arrangement of measurement points in hardness test after surfacing

Analysis of Test Results

The technological tests revealed that the process of plasma–powder surfacing was very stable within the entire range of parameters used and that the overlay welds obtained were characterised by smoothness and equal width as well as were free from surface impurities. The macroscopic metallographic tests revealed that the individual overlay welds differed in width, height, and primarily, in the penetration depth and the base material content. The characteristic features mentioned above were affected by surfacing process technological parameters and in particular by the powder mass feeding rate, current and surfacing rate.

The tests revealed that the powder mass feeding rate primarily affected the overlay weld height and the content of the base material in the overlay weld. However, the powder mass feeding rate did not affect the penetration depth or the overlay weld width. At constant current, an increase in the powder mass feeding rate caused an increase in the overlay weld height and a decrease in the percentage content of the base material in the overlay weld. The macroscopic metallographic tests of the overlay welds made using higher values of plasma arc current (120 A and 150 A) revealed that increasing the

Table 2. Hardness measurement results for overlay welds and HAZ

Specimen no. acc. to description	Hardness in measurement point according to Figure 14, HV10																	
	1	2	3	4	5	6	7	8	9	10	11	12	13	14	15	16	17	18
1	290	301	311	306	307	298	301	311	297	129	150	161	310	295	251	152	155	151
3	270	301	307	308	303	308	300	302	279	159	170	162	300	274	230	154	153	153
6	336	375	380	377	376	389	379	384	375	157	165	166	380	302	243	167	163	161
8	384	391	403	398	395	395	403	404	397	175	187	176	390	329	219	159	152	154
34	242	250	256	257	260	254	256	254	249	154	169	158	257	243	221	159	159	159
38	360	398	401	409	403	406	401	399	396	152	163	165	359	249	178	154	151	153
40	373	393	382	395	398	391	381	393	373	153	157	152	337	266	190	165	154	152
27	357	410	404	407	396	399	398	404	373	164	185	182	404	368	292	152	150	150
31	316	373	354	359	371	370	364	373	330	143	158	157	345	263	174	160	155	155
33	279	307	304	325	296	326	322	333	397	137	152	160	226	168	155	155	156	155

Specimen designations:

Specimens no. 1, 3, 6, 8:

current 100 A, surfacing rate 20 cm/min, powder mass feeding rate 5 g/min (1 and 6) and 8,72 g/min (3 and 8) respectively, specimens 1 and 3 made with preheating to 200 C, specimens 6 and 8 surfaced without preheating;

Specimens no. 34, 38, 40:

current 120 A, powder mass feeding rate 10.64 g/min, surfacing rate: 10 cm/min (34), 30 cm/min (38) and 40 cm/min (40) respectively;

Specimens no. 27, 31, 33:

Surfacing rate 30 cm/min, powder mass feeding rate 10.64 g/min, current: 90 A (27), 120 A (31) and 150 A (33) respectively

powder mass feeding rate two times increased the overlay weld thickness almost two times as well as increased the base material content by approximately 40%. Figure 15 presents the effect of the powder mass feeding rate on the overlay weld height, whereas Figure 16 presents the effect of the powder mass feeding rate on the content of the base material in the overlay weld.

The analysis of the test results revealed that a surfacing rate increased from 10 to 105 cm/min, at a constant powder mass feeding rate and constant current decreased the overlay weld width almost three times and the overlay weld height almost four times (Table 6). The penetration depth decreased as well but this was due to decreases in the remaining geometric parameters of the overlay weld; the content of the base material in the overlay weld changed irregularly within the range of approximately 30-60%. Figure 17 presents the effect of a surfacing rate on the overlay weld width, whereas Figure 18 presents the effect of a surfacing rate on the overlay weld height.

The measurements of overlay weld geometry and penetration depth as well as the calculations determining the content of the base material in the overlay weld revealed that current had the greatest effect on the characteristics mentioned above. Current increased from 80 A to 150 A at a constant surfacing rate of 30 cm/min and a constant powder mass feeding rate of 10.64 g/min caused an increase in the overlay weld width and a decrease in the overlay weld height by approximately 30%. However, the greatest changes were concerned with the penetration depth and the content of the base material in the overlay weld.

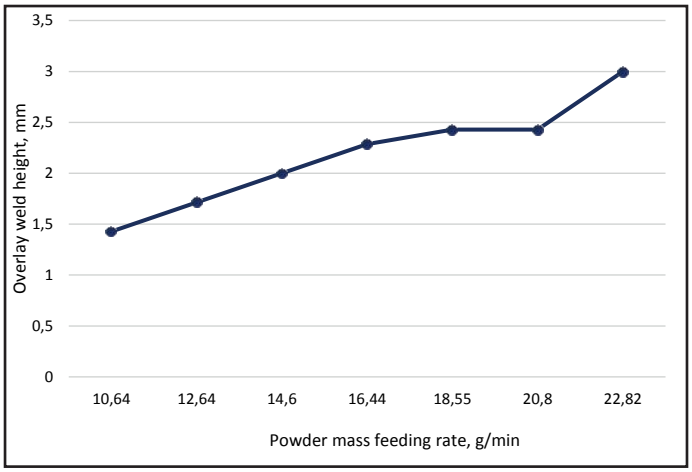

Fig. 15. Diagram presenting the dependence of the overlay weld height on powder mass feeding rate at constant welding current (120 A) and constant surfacing rate (20 cm/min)

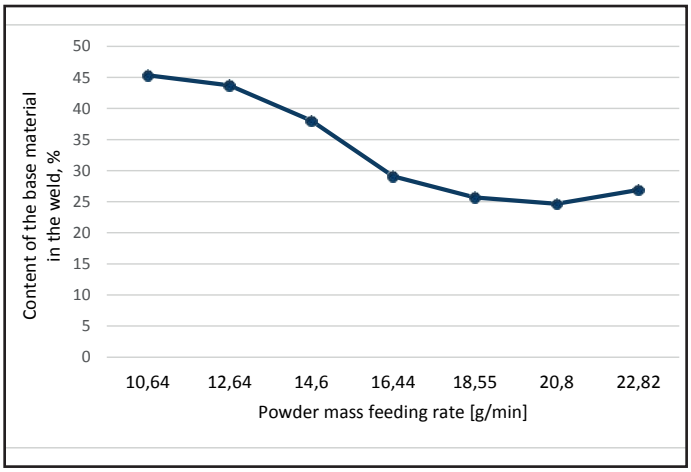

Fig. 16. Diagram presenting the dependence of the content of the base material in the overlay weld on powder mass feeding rate at constant welding current (120 A) and constant surfacing rate (20 cm/min)

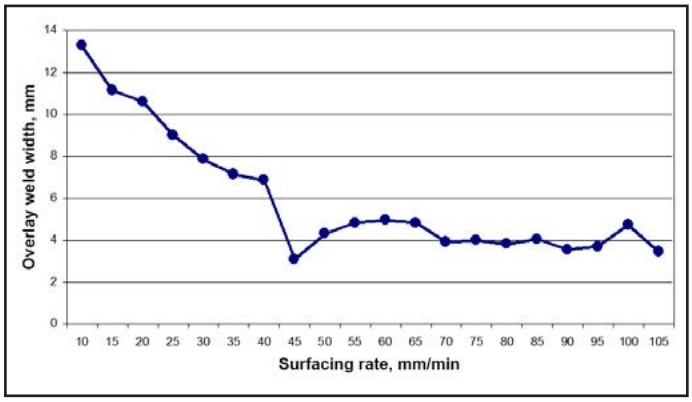

Fig. 17. Diagram presenting the dependence of the overlay weld width on surfacing rate at constant welding current (120 A) and constant powder mass feeding rate (10.64 g/min)

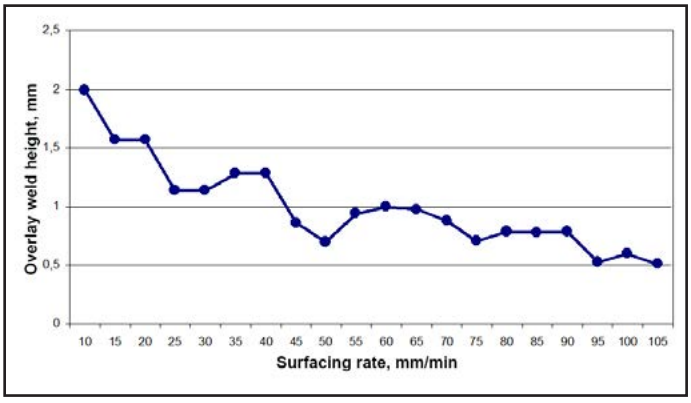

Fig. 18. Diagram presenting the dependence of the overlay weld height on surfacing rate at constant welding current (120 A) and constant powder mass feeding rate (10.64 g/min)

The tests revealed that in the conditions presented above the penetration depth increased five times, and the content of the base material in the overlay weld increased almost three times. The results are presented graphically in Figures 19 and 20.

The microscopic metallographic tests performed using a light microscope revealed that the HAZ structure of elements after surfacing was complex. The areas located farther from the fusion line were characterised by a refined ferritic-pearlitic structure. Areas located closer to the fusion line contained bainite and martensite, whereas areas located at the direct vicinity of the fusion line were characterised by significant grain growth (Figures 7-8, 10-11). The overlay weld structure was austenitic, characteristic of nickel alloys (Figures 9 and 12). Images revealed a characteristic (dendritic) overlay weld structure. The tests revealed that the powder mass feeding rate did not affect the structure of the HAZ and that of the overlay weld. The HAZ width remained the same, the amount of bainite and martensite in the structure was similar and so was the grain size. In turn, the structure was affected by surfacing current. In the HAZ, it was possible to observe significantly greater grain sizes and a greater amount of martensite. The overlay weld structure remained practically unchanged. The HAZ structure after surfacing was also affected by the use of preheating. Elements preheated to 200°C revealed structure refinement and less martensite.

The hardness measurements revealed that the highest values (even above 400 HV) characterised the HAZ areas located directly under the overlay weld (points 4, 5 and 6, Fig. 14, Table 2). Slightly lower hardness values were measured on the overlay weld edges, and the lowest hardness values were present in the overlay weld. The tests revealed that hardness in the individual HAZ areas was affected by surfacing current, welding rate and the use of preheating. Increased current reduced the HAZ hardness from the maximum value of 410 HV (90A)

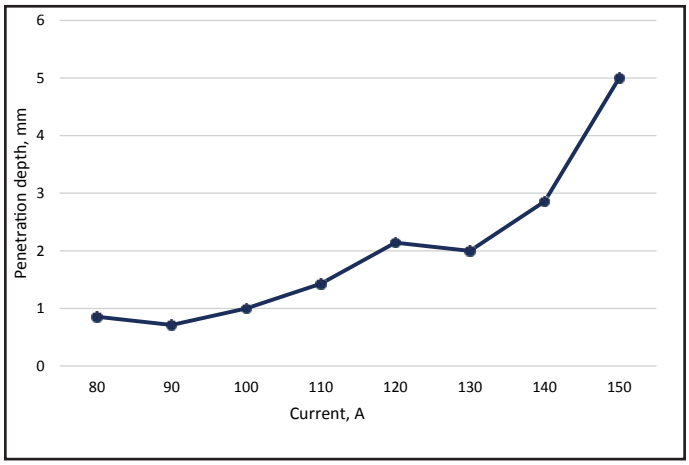

Fig. 19. Diagram presenting the dependence of the penetration depth on welding current at constant powder mass feeding rate (10.64 g/min) and constant surfacing rate (30 cm/min)

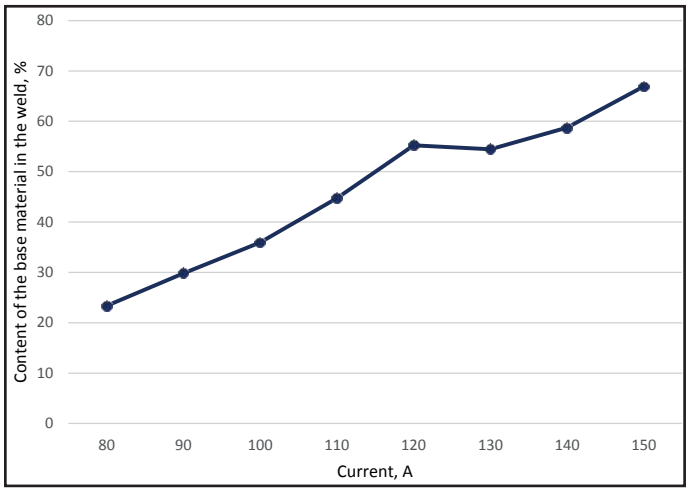

Fig. 20. Diagram presenting the dependence of the content of the base material in the overlay weld on welding current at constant powder mass feeding rate (10.64 g/min) and constant surfacing rate (30 cm/min)

to 307 HV (150 A). In turn, increased surfacing rates increased hardness from the value of 260 HV (10 cm/min) to 393 HV (40 cm/min). The assessment criterion applied when evaluating hardness test results for steels of group 5.2 according to ISO TR 15608 (chromium–molybdenum steels) is the obtainment of values below 380 HV (requirement formulated in PN-EN ISO 15614-1:2008/A2:2012). In the case of low current (approximately 100 A) and a high surfacing rate (above 20 cm/min) it is necessary to use preheating as this procedure significantly reduces hardness in the HAZ. To this end, it is also possible to use low surfacing rates and high current, yet when developing a surfacing technology it is necessary to take into consideration

overlay weld geometry, the degree of stirring with the base material, penetration depth and HAZ width. The parameters used should enable the obtainment of requirements in terms of layer thickness and the degree of stirring with the base material as well as requirements related to material hardness after surfacing.

Summary and conclusions

The tests revealed that the plasma–powder surfacing of 10CrMo9-10 steel using a Eutronic GAP 3001 device and Inconel 625 powder was very stable within the entire range of parameters tested and that the overlay welds obtained were characterised by very good quality. The technological process parameters (primarily powder mass feeding rate, current and welding rate) affected overlay weld geometry, penetration depth and the content of the base material in the overlay weld. It was possible to adjust individual parameters in order to obtain a required overlay weld shape, required penetration depth and the proper content of the base material in the overlay weld, making it possible to maintain specific overlay weld properties, e.g. resistance to corrosion or to abrasive wear. Technological parameters such as current and surfacing rate also affected the material hardness in the HAZ. Hardness was also affected by the use of preheating. When developing a surfacing technology, in addition to overlay weld geometry and overlay weld-base material stirring degree, it is also necessary to allow for the effect of technological parameters on the structure, and, consequently, hardness.

The technological tests of plasma–powder surfacing and the metallographic tests of elements after surfacing, as well as the analysis of results obtained enabled the formulation of the following conclusions:

1. The proper adjustment of technological parameters (powder mass feeding rate, current and surfacing rate) make it possible to shape overlay weld geometry and affect the base material content in the overlay weld as needed.

2. An increase in powder mass feeding rate increases the overlay weld height and reduces the base material content. A 50% increase in current increases penetration depth and the base material content (in the overlay weld) several times.

3. Technological parameters, particularly surfacing rate and surfacing current, as well as the use of preheating affect the structure and hardness of the overlay weld and of the HAZ. An increase in welding rate, or a decrease in current, increases hardness.

References

[1] Klimpel A.: Technologie napawania i natryskiwania cieplnego. Wydawnictwo Politechniki Śląskiej, Gliwice, 1999

[2] Adamiec P., Dziubiński J., Adamiec J.: Napawanie elementów wymienników ciepła w kotłach do spalania odpadów. Spajanie, 2006, no. 3

[3] Jarosiński J., Błaszczyk M., Tasak E.: Napawanie stali stosowanych w energetyce stopami na osnowie niklu. Przegląd Spawalnictwa, 2007, no. 1

[4] Kik T., Górka J., Czupryński A.: Napawanie plazmowe proszkowe stali energetycznej 16Mo3. Spajanie, 2010, nos. 3-4